Activation of ACE2 and interferon-stimulated transcriptomes in human airway epithelium is curbed by Janus Kinase inhibitors

Hye Kyung Lee[1], Olive Jung[2], and Lothar Hennighausen[1]

[1]Laboratory of Genetics and Physiology, National Institute of Diabetes, Digestive and Kidney Diseases, National Institutes of Health, Bethesda, Maryland 20892.
[2]Division of Preclinical Innovation, National Center for Advancing Translational Sciences, National Institutes of Health, Rockville, Maryland 20850.

Abstract

SARS-CoV-2 infection of human airway epithelium activates genetic programs that lead to progressive hyperinflammation in COVID-19 patients. Here we report on the transcriptomic response of airway epithelium to interferons and its suppression by the JAK inhibitors Baricitinib and Ruxolitinib. There is a debate on the regulation of the conventional versus the novel intronic promoter inducing the short *ACE2* isoform. Through RNA-seq and ChIP-seq analyses for activating chromatin marks and Polymerase II, we define the interferon-activated intronic regulatory region. Our results also support that the conventional *ACE2* promoter is controlled by interferon.

Introduction

The angiotensin-converting enzyme 2 (ACE2) receptor is the gateway for SARS-CoV-2 to airway epithelium[1,2] and the strong inflammatory response after viral infection is a hallmark in COVID-19 patients. Janus kinase (JAK) inhibitors are used therapeutically to harness cytokine storms[3,4] because they suppress signal transduction pathways that lead to immune activation and inflammation. However, the genetic programs activated in airway cells by interferons and their response to JAK inhibitors remain to be elucidated. In addition, there is a current debate on the regulation of the SARS-CoV-2 receptor ACE2 by interferons and the functional consequences[5-8].

Results

In a quest to comprehensively identify transcriptomes activated in human airway epithelium by cytokines, we focused on the well-established primary Small Airway Epithelial Cells (SAEC) that express a wide range of cytokine receptors and key mechanistic components of the JAK/STAT signal transduction pathway (Supplementary Table 1). We stimulated SAECs with interferon type 1 (IFNα and IFNβ), type II (IFNγ) and type III (IFNλ) as well as with growth hormone (GH), Interleukin 6 (IL6) and IL7, followed by RNA-seq analyses (Supplementary Tables 2-8). Cytokine treatment resulted in a more than 2-fold activation of 1405 genes (IFNα), 647 (IFNβ), 1570 (IFNγ), 1285 (IFNλ3), 1432 (IL6), 1782 (IL7) and 2807 (GH), significantly. A total of 229 genes were activated by all four interferons, and three genes (IRF7, IFI27, IFI35 and PARP10) were induced by all seven cytokines.

Depending on the interferon, between 17% and 26% of the induced genes were linked to immune responses (Figure 1a and 1b). Among them are interleukins, Interferon Stimulated Genes (ISG), IFIT family members and IRF transcription factors (Supplementary Figure 1). Levels of the transcription factor STAT1, which itself is a major driver of immune response and contributes to the pathogenesis of coronavirus infections[9], were increased more than 20-fold by any of the interferons (Supplementary Figure 1), likely through a JAK/STAT dependent enhancer. For most of these genes, key regulatory elements, such as enhancers, have not been identified. To facilitate the annotation of regulatory elements associated with interferon-induced genes, we conducted ChIP-seq experiments for chromatin marks H3K4me3 (promoter marks), HeK4me1 (enhancer marks) and H3K27ac (active loci) as well as for RNA Polymerase (Pol) II and MED1 (enhancers). These data sets permit the identification of regulatory elements (examples in Supplementary Figure 2).

JAK inhibitors suppress cytokine-induced gene activation through the JAK/STAT pathway and are used to manage cytokine storms in COVID-19 patients[3,4]. To clarify the dependence of IFNβ-induced transcriptome on the JAK/STAT pathway, we employed two JAK inhibitors, Baricitinib and Ruxolitinib (inhibiting JAK1 and JAK2), that are in COVID-19 clinical trials[10]. SAEC were cultured in the presence of IFNβ and either Baricitinib or Ruxolitinib, followed by RNA-seq analyses (Supplementary Tables 9 and 10). Both inhibitors led to a suppression of IFNβ-induced gene activation (Figure 1c). While for

some genes, expression was completely blunted, for others the suppression was incomplete (Supplementary Tables 10 and 11). qRT-PCR for STAT1 and the SARS-CoV-2 receptor ACE2 validated suppression to baseline levels, i.e. expression seen without cytokine stimulation (Supplementary Figure 3a) and immune-associated genes were also inhibited by the inhibitors (Supplementary Figure 3b-d).

ACE2 is the receptor for SARS-CoV-2 and a recent single-cell RNA-seq study[5] determined that type I IFNs upregulate *ACE2* expression through a putative promoter and a putative distal binding site for STAT transcription factors. It was suggested that this increase could result in a higher infectivity of airway epithelium, the main entry point of the virus. Since single-cell RNA-seq approaches have a restricted read depth, they are suboptimal for detecting isoforms of low-abundance transcripts, such as *ACE2*. Very recent studies using bulk RNA-seq data[7,8] and a cancer transcriptome analysis[6] led to the discovery of a novel short form of ACE2 (dACE2) which originates from an interferon-responsive co-opted retroviral promoter within intron 9 of the *ACE2* gene. Our RNA-seq data demonstrated a more than 20-fold increase of *ACE2* mRNA levels upon in IFNα/β treated SAEC and confirmed the presence of the novel exon 1c, likely controlled by its own promoter (Figure 2a). To obtain more definitive information on the interferon regulation of the respective promoters, we determined the read counts of the three exons (1a, 1b and 1c) are associated with different promoters (Figure 2b). While the increase of RNA-seq reads induced by IFNα/β was highest (~10-fold) over exon 1c, a lesser, yet significant, ~3-5-fold increase was detected over exons 1a and 1b, supporting the notion that interferons induce expression of the full-length *ACE2* isoform. JAK inhibitor experiments further supported that these promoters are under control of the JAK/STAT pathway (Figure 2c). Activation of the novel *ACE2* promoter and transcription of exon 1c was observed with all interferons tested but not with other cytokines (Supplementary Figure 4).

To clarify the nature of regulatory elements controlling transcription of the two *ACE2* isoforms, we dug deeper and interrogated our ChIP-seq data sets for H3K27ac (activating mark), H3K4me1 (enhancer mark), H3K4me3 (promoter mark), binding of MED1 and Polymerase II (Pol II) loading, both in the absence and presence of IFNβ (Figure 2d). While the *bona fide ACE2* promoters at exons 1a and 1b displayed few

histone marks and Pol II binding, strong coverage was observed in intron 9 adjacent to exon 1c (Figure 2d and 2e). H3K27ac, H3K4me3 and Pol II loading were further induced upon IFNβ treatment. *BCL6* was used a control gene. ChIP-seq experiments from K562 erythroid cells stimulated with IFNβ[11] revealed binding of STAT1, STAT2 and STAT5 to the intronic promoter/enhancer (Figure 2f). IFNβ induced binding of the three STAT members was observed at the STAT1 gene.

Discussion

Our study not only provided structural and mechanistic evidence to support the intronic promoter/enhancer that controls expression of the *dACE2* transcript, but it also corroborates previous findings that the conventional *ACE2* promoters at the 5' exons are under interferon control[5], possibly through a distal enhancer. The intronic regulatory element appears to be an evolutionary remnant of an LTR[6], and it is not uncommon for endogenous proviruses or their vestiges to be activated by cytokines with the ensuing RNA polymerase picking up hitchhiking exons along its path of transcription[12]. Regulation of the human and mouse *ACE2*[13] locus displays distinct differences, yet they share their responsiveness to cytokines and the JAK/STAT pathway. The mouse *Ace2* gene is activated in mammary tissue by cytokines through a JAK2/STAT5-dependent intronic enhancer, which is not apparent in the human gene in airway cells. Further studies are needed to understand the complex, possibly cell-specific, regulation of the human *ACE2* locus in tissues with extrapulmonary manifestations of COVID-19 infection.

Materials and Methods

Cell culture

Human small airway epithelial cells (SAEC) obtained from Lifeline Technology (FC-0016) were expanded using the complete BronchiaLife™ media kit (Lifeline Technology, LL-0023). All culture wares were pre-coated in 30 ug/ml of Fibronectin (ThermoFisher Scientific, 33016015) for at least 1h at room temperature. Calu-3 line (ATCC, HTB-55™) were cultured using Eagle's Minimum Essential Medium (ATCC, 30-2003™) containing 10% fetal bovine serum (Cytiva, SH3007103) in 5% CO2 atmosphere at 37°C.

Cytokines (10 ng/ml; Human IFNβ, 300-02BC; Human IFNγ, 300-02; Human IL6, 200-06; Human IL7, 200-07; Human Growth hormone, 100-40, Peprotech; Human IFNα2b, 78077.1, Stem Cell Technologies; Human IFNλ3, 5259-IL-025, R&D systems) were treated in respective culture media and the cells were incubated for 12h in 5% CO2 atmosphere at 37°C. The cells were washed with PBS (Gibco, 14190144) twice and harvested.

Jak inhibitors, 10 uM of either Baricitinib (HY-15315A, MedChemExpress) or Ruxolitinib (HY-50856A, MedChemExpress), were treated in BronchiLiafe™ media with or without IFNb treated SAEC and incubated for overnight. The cells were then washed with PBS twice and harvested.

RNA isolation and quantitative real-time PCR (qRT–PCR)

Mammary tissues were harvested from non-parous and day 10 of lactating female mice and homogenized using an electronic homogenizer. RNA was extracted using the PureLink RNA Mini Kit (Invitrogen) according to the manufacturer's instructions. cDNA was synthesized from total RNA using Superscript II (Invitrogen). Quantitative real-time PCR (qRT-PCR) was performed using TaqMan probes (ACE2, Hs01085333_m1; TMPRSS2, Hs01122322_m1; *STAT1*, Hs01013996_m1; STAT3, Hs00374280_m1; STAT5B, Hs00560026_m1; JAK1, Hs01026983_m1; JAK3, Hs00354555_m1; *GAPDH*, Hs02786624_g1, Thermo Fisher scientific) on the CFX384 Real-Time PCR Detection System (Bio-Rad) according to the manufacturer's instructions. PCR conditions were 95°C for 30s, 95°C for 15s, and 60°C for 30s for 40 cycles. All reactions were done in triplicate and normalized to the housekeeping gene *Gapdh*. Relative differences in PCR results were calculated using the comparative cycle threshold (C_T) method.

Total RNA sequencing (Total RNA-seq) and data analysis.

Total RNA was extracted from the collected cells and purified with RNeasy Plus Mini Kit (Qiagen, 74134). Ribosomal RNA was removed from 1 µg of total RNAs and cDNA was synthesized using SuperScript III (Invitrogen). Libraries for sequencing were prepared according to the manufacturer's instructions with TruSeq Stranded Total RNA Library Prep Kit with Ribo-Zero Gold (Illumina, RS-122-2301) and paired-end sequencing was

done with a HiSeq 2500 instrument (Illumina).

Total RNA-seq read quality control was done using Trimmomatic [14] (version 0.36) and STAR RNA-seq [15] (version STAR 2.5.4a) using 50bp paired-end mode was used to align the reads (hg19). HTSeq [16] was to retrieve the raw counts and subsequently, R (https://www.R-project.org/), Bioconductor [17] and DESeq2 [18] were used. Additionally, the RUVSeq [19] package was applied to remove confounding factors. The data were pre-filtered keeping only those genes, which have at least ten reads in total. Genes were categorized as significantly differentially expressed with an adjusted p-value (pAdj) below 0.05 and a fold change > 2 for up-regulated genes and a fold change of < -2 for down-regulated ones. The visualization was done using dplyr (https://CRAN.R-project.org/package=dplyr) and ggplot2 [20]. Sequence read numbers were calculated using Samtools[21] software with sorted bam files.

Chromatin immunoprecipitation sequencing (ChIP-seq) and data analysis.

Chromatin was fixed with formaldehyde (1% final concentration) for 15 min at room temperature, and then quenched with glycine (0.125 M final concentration). Samples were processed as previously described[22]. The following antibodies were used for ChIP-seq: STATq (Santa Cruz Biotechnology, sc-), MED1 (Bethyl Laboratory, A300-793A), H3K27ac (Abcam, ab4729), RNA polymerase II (Abcam, ab5408), H3K4me1 (Active Motif, 39297) and H3K4me3 (Millipore, 07-473). Libraries for next-generation sequencing were prepared and sequenced with a HiSeq 2500 or 3000 instrument (Illumina). Quality filtering and alignment of the raw reads was done using Trimmomatic[14] (version 0.36) and Bowtie[23] (version 1.1.2), with the parameter '-m 1' to keep only uniquely mapped reads, using the reference genome hg19. Picard tools (Broad Institute. Picard, http://broadinstitute.github.io/picard/. 2016) was used to remove duplicates and subsequently, Homer[24] (version 4.8.2) software was applied to generate bedGraph files. Integrative Genomics Viewer[25] (version 2.3.81) was used for visualization.

Statistical anlaysis

For comparison of samples, data were presented as standard deviation in each group and were evaluated with a two-way ANOVA followed by Tukey's multiple comparisons

test using PRISM GraphPad. Statistical significance was obtained by comparing the measures from wild-type or control group, and each mutant group. A value of $*P < 0.05$, $**P < 0.001$, $***P < 0.0001$, $****P < 0.00001$ was considered statistically significant.

Data availability. ChIP-seq for STATs was obtained under GSE31477. The RNA-seq and ChIP-seq data from SAEC will be uploaded in GEO before publishing the manuscript.

Acknowledgments

We thank Ilhan Akan, Sijung Yun and Harold Smith from the NIDDK genomics core for NGS and NCATS Chemical Genomics Center Team for the JAK inhibitors. This work utilized the computational resources of the NIH HPC Biowulf cluster (http://hpc.nih.gov).

Funding

This work was supported by the Intramural Research Programs (IRPs) of National Institute of Diabetes and Digestive and Kidney Diseases (NIDDK) and National Center for Advancing Translational Sciences (NCATS).

Author contribution

HKL: project conception, experimental design and execution, data analysis, preparation of figures, writing manuscript; OJ: experimental design and execution; LH: project conception, experimental design, data analysis, preparation of figures, writing manuscript.

Competing interests

The authors declare no competing financial interests.

References

1. Hoffmann, M. *et al.* SARS-CoV-2 Cell Entry Depends on ACE2 and TMPRSS2 and Is Blocked by a Clinically Proven Protease Inhibitor. *Cell* **181**, 271-280 e8 (2020).
2. Lukassen, S. *et al.* SARS-CoV-2 receptor ACE2 and TMPRSS2 are primarily expressed in bronchial transient secretory cells. *EMBO J*, e105114 (2020).

3. La Rosee, F. *et al.* The Janus kinase 1/2 inhibitor ruxolitinib in COVID-19 with severe systemic hyperinflammation. *Leukemia* **34**, 1805-1815 (2020).
4. Spinelli, F.R., Conti, F. & Gadina, M. HiJAKing SARS-CoV-2? The potential role of JAK inhibitors in the management of COVID-19. *Sci Immunol* **5**(2020).
5. Ziegler, C.G.K. *et al.* SARS-CoV-2 Receptor ACE2 Is an Interferon-Stimulated Gene in Human Airway Epithelial Cells and Is Detected in Specific Cell Subsets across Tissues. *Cell* (2020).
6. Ng, K. *et al.* Tissue-specific and interferon-inducible expression of non-functional ACE2 through endogenous retrovirus co-option. *bioRxiv*, 2020.07.24.219139 (2020).
7. Onabajo, O.O. *et al.* Interferons and viruses induce a novel primate-specific isoform dACE2 and not the SARS-CoV-2 receptor ACE2. *bioRxiv* (2020).
8. Blume, C. *et al.* A novel isoform of ACE2 is expressed in human nasal and bronchial respiratory epithelia and is upregulated in response to RNA respiratory virus infection. *bioRxiv*, 2020.07.31.230870 (2020).
9. Page, C. *et al.* Induction of alternatively activated macrophages enhances pathogenesis during severe acute respiratory syndrome coronavirus infection. *J Virol* **86**, 13334-49 (2012).
10. ClinicalTrials.gov (https://clinicaltrials.gov/ct2/results?cond=covid-19&term=ruxolitinib&cntry=&state=&city=&dist=)
11. Au-Yeung, N., Mandhana, R. & Horvath, C.M. Transcriptional regulation by STAT1 and STAT2 in the interferon JAK-STAT pathway. *JAKSTAT* **2**, e23931 (2013).
12. Stegalkina, S.S. *et al.* Transcription originating in the long terminal repeats of the endogenous mouse mammary tumor virus MTV-3 is activated in Stat5a-null mice and picks Up hitchhiking exons. *J Virol* **73**, 8669-76 (1999).
13. Hennighausen, L. & Lee, H.K. Activation of the SARS-CoV-2 Receptor Ace2 through JAK/STAT-Dependent Enhancers during Pregnancy. *Cell Rep*, 108199 (2020).
14. Bolger, A.M., Lohse, M. & Usadel, B. Trimmomatic: a flexible trimmer for Illumina sequence data. *Bioinformatics* **30**, 2114-20 (2014).

15. Dobin, A. *et al.* STAR: ultrafast universal RNA-seq aligner. *Bioinformatics* **29**, 15-21 (2013).
16. Anders, S., Pyl, P.T. & Huber, W. HTSeq--a Python framework to work with high-throughput sequencing data. *Bioinformatics* **31**, 166-9 (2015).
17. Huber, W. *et al.* Orchestrating high-throughput genomic analysis with Bioconductor. *Nat Methods* **12**, 115-21 (2015).
18. Love, M.I., Huber, W. & Anders, S. Moderated estimation of fold change and dispersion for RNA-seq data with DESeq2. *Genome Biol* **15**, 550 (2014).
19. Risso, D., Ngai, J., Speed, T.P. & Dudoit, S. Normalization of RNA-seq data using factor analysis of control genes or samples. *Nat Biotechnol* **32**, 896-902 (2014).
20. Wickham, H. *Ggplot2 : elegant graphics for data analysis*, viii, 212 p. (Springer, New York, 2009).
21. Masella, A.P. *et al.* BAMQL: a query language for extracting reads from BAM files. *BMC Bioinformatics* **17**, 305 (2016).
22. Metser, G. *et al.* An autoregulatory enhancer controls mammary-specific STAT5 functions. *Nucleic Acids Res* **44**, 1052-63 (2016).
23. Langmead, B., Trapnell, C., Pop, M. & Salzberg, S.L. Ultrafast and memory-efficient alignment of short DNA sequences to the human genome. *Genome Biol* **10**, R25 (2009).
24. Heinz, S. *et al.* Simple combinations of lineage-determining transcription factors prime cis-regulatory elements required for macrophage and B cell identities. *Mol Cell* **38**, 576-89 (2010).
25. Thorvaldsdottir, H., Robinson, J.T. & Mesirov, J.P. Integrative Genomics Viewer (IGV): high-performance genomics data visualization and exploration. *Brief Bioinform* **14**, 178-92 (2013).

Figure legends

Figure 1. Activation of immune response genes by Interferons in human primary airway epithelium (SAEC). a. Genes induced significantly by IFNα, β, γ and λ3 were significantly enriched in Hallmark Gene Sets (FDR q-value < 0.005). Immune response genes accounted for 18.4%, 26.3%, 20.1% and 17% of the upregulated genes. **b.** Expression of each immune response was displayed by heatmaps. **c.** Expression of immune pathway genes induced by IFNβ was diminished by the JAK inhibitors.

Figure 2. Activation of the novel intronic and the classical *ACE2* promoters by IFNβ through the JAK-STAT pathway. a. IGV plot displays RNA reads mapped at *ACE2* locus from control and IFNα/β treated SAEC. The *CELF1* gene severed as a control. **b-c.** Number of RNA reads at the exons 1a and 1b, and the new exon 1c. SAECs were grown in the absence of interferons (control) and in the presence of IFNα/β with and without JAK inhibitors, Baricitinib or Ruxolitinib. Results are shown as the means ± SEM. of independent biological replicates (n = 3). **d-e.** ChIP-seq data for MED1, Pol II and histone markers H3K27ac, H3K4me1 and H3K4me3 at the *ACE2* locus in SAECs with and without IFNβ. Solid arrows indicate the orientation of genes. The orange and blue shades indicate regulatory elements. The *BCL6* gene served as a ChIP-seq control. **f.** Putative STAT5 enhancers in the *ACE2* gene were identified using ChIP-seq data from IFNβ treated K562 cells.

Supplementary Figure 1. Interferon induced distinct immune pathway. a-f. Comparison of relative normalized gene expression levels of representative genes from the interferon response of Hallmark Gene Sets between control (n=4) and experimental (n=3) groups. Results are shown as the means ± SEM. of independent biological replicates. Multiple sample pairs were analyzed with two-way ANOVA followed by Tukey's multiple comparisons test (GraphPad Prism). *P < 0.05, **P < 0.001, ***P < 0.0001, ****P < 0.00001.

Supplementary Figure 2. Regulatory features of IFNβ-induced genes. ChIP-seq data for MED1, RNA Pol II and histone markers H3K27ac, H3K4me1 and H3K4me3 provided

structural information about the loci of immune genes highly induced by IFNβ. Solid arrows indicate the orientation of genes.

Supplementary Figure 3. JAK inhibitors suppressed activation of IFNβ-induced genes. a. *ACE2* and *STAT1* mRNA levels from control and experimental cells were measured by qRT–PCR and normalized to *GAPDH* levels. Results are shown as the means ± s.e.m. of independent biological replicates (n = 3). Two-way ANOVA followed by Tukey's multiple comparisons test was used to evaluate the statistical significance of differences. **b-d.** Comparison of relative normalized gene expression levels of genes induced by IFNβ (Supplementary Figure 1) from the interferon response-related Hallmark Gene Sets between control (n=4) and IFNs (n=3) groups. Results are shown as the means ± SEM. of independent biological replicates. Multiple sample pairs were analyzed with two-way ANOVA followed by Tukey's multiple comparisons test (GraphPad Prism). *P < 0.05, **P < 0.001, ***P < 0.0001, ****P < 0.00001.

Supplementary Figure 4. A novel short transcript of *ACE2* was induced by interferons but not by other cytokines. IGV plot displays RNA reads covering the entire *ACE2* gene from control and experimental SAECs. The *CELF1* severed as a control.

Supplementary Table 1. mRNA levels of genes associated with the pan JAK-STAT pathway in SAEC.

Supplementary Table 2. List of all genes with normalized read counts in each replicate at Control and IFNα treated SAEC, $\log_2$ (fold change), p-value and adjusted p-value as well as upregulated gene list and GSEA analysis.

Supplementary Table 3. List of all genes with normalized read counts in each replicate at Control and IFNβ treated SAEC, $\log_2$ (fold change), p-value and adjusted p-value as well as upregulated gene list and GSEA analysis.

Supplementary Table 4. List of all genes with normalized read counts in each replicate at Control and IFNγ treated SAEC, log_2 (fold change), *p*-value and adjusted *p*-value as well as upregulated gene list and GSEA analysis.

Supplementary Table 5. List of all genes with normalized read counts in each replicate at Control and IFNλ3 treated SAEC, log_2 (fold change), *p*-value and adjusted *p*-value as well as upregulated gene list and GSEA analysis.

Supplementary Table 6. List of all genes with normalized read counts in each replicate at Control and IL6 treated SAEC, log_2 (fold change), *p*-value and adjusted *p*-value as well as upregulated gene list and GSEA analysis.

Supplementary Table 7. List of all genes with normalized read counts in each replicate at Control and IL7 treated SAEC, log_2 (fold change), *p*-value and adjusted *p*-value as well as upregulated gene list and GSEA analysis.

Supplementary Table 8. List of all genes with normalized read counts in each replicate at Control and GH treated SAEC, log_2 (fold change), *p*-value and adjusted *p*-value as well as upregulated gene list and GSEA analysis.

Supplementary Table 9. List of all genes with normalized read counts in each replicate at IFNβ and Baricitinib with IFNβ, treated SAEC, log_2 (fold change), *p*-value and adjusted *p*-value as well as upregulated gene list and GSEA analysis.

Supplementary Table 10. List of all genes with normalized read counts in each replicate at IFNβ and Ruxolitinib with IFNβ, treated SAEC, log_2 (fold change), *p*-value and adjusted *p*-value as well as upregulated gene list and GSEA analysis.

Supplementary Table 11. List of all genes with normalized read counts in each replicate at Control and Jak inhibitor, Baricitinib, treated SAEC, log_2 (fold change), *p*-value and adjusted *p*-value as well as upregulated gene list and GSEA analysis.

Supplementary Table 12. List of all genes with normalized read counts in each replicate at Control and Jak inhibitor, Ruxolitinib, treated SAEC, $\log_2$ (fold change), *p*-value and adjusted *p*-value as well as upregulated gene list and GSEA analysis.

Figure 1

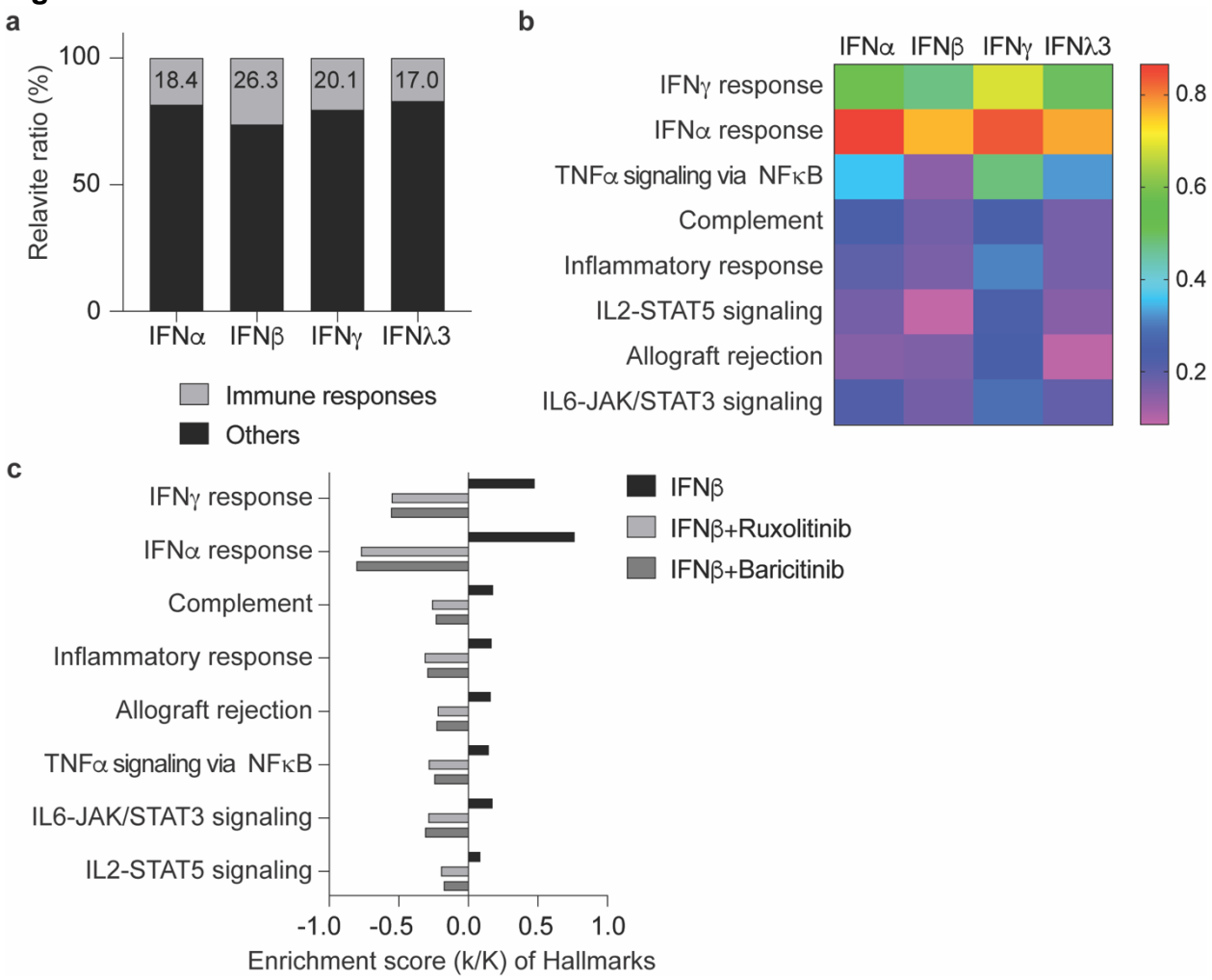
a
Relavite ratio (%)
100
50
0
18.4
26.3
20.1
17.0
IFNα
IFNβ
IFNγ
IFNλ3
Immune responses
Others
b
IFNα
IFNβ
IFNγ
IFNλ3
IFNγ response
IFNα response
TNFα signaling via NFκB
Complement
Inflammatory response
IL2-STAT5 signaling
Allograft rejection
IL6-JAK/STAT3 signaling
0.8
0.6
0.4
0.2
c
IFNγ response
IFNα response
Complement
Inflammatory response
Allograft rejection
TNFα signaling via NFκB
IL6-JAK/STAT3 signaling
IL2-STAT5 signaling
-1.0
-0.5
0.0
0.5
1.0
Enrichment score (k/K) of Hallmarks
IFNβ
IFNβ+Ruxolitinib
IFNβ+Baricitinib

Figure 2

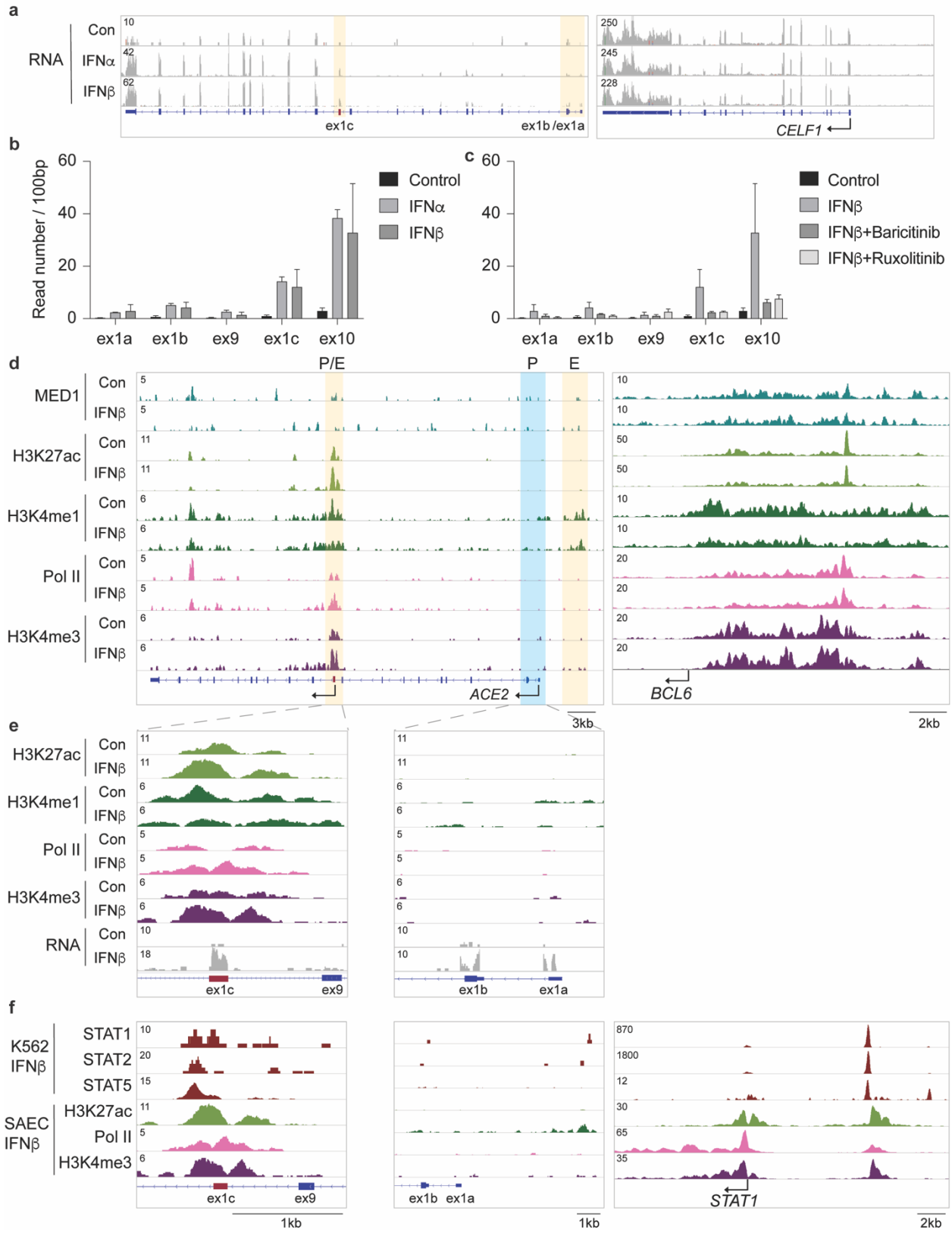
a
RNA
Con
IFNα
IFNβ
ex1c
ex1b /ex1a
CELF1
b
Read number / 100bp
Control
IFNα
IFNβ
ex1a
ex1b
ex9
ex1c
ex10
c
Control
IFNβ
IFNβ+Baricitinib
IFNβ+Ruxolitinib
d
P/E
P
E
MED1
H3K27ac
H3K4me1
Pol II
H3K4me3
ACE2
BCL6
3kb
2kb
e
RNA
ex1c
ex9
ex1b
ex1a
f
K562 IFNβ
STAT1
STAT2
STAT5
SAEC IFNβ
1kb
2kb

Supplementary Figure 1

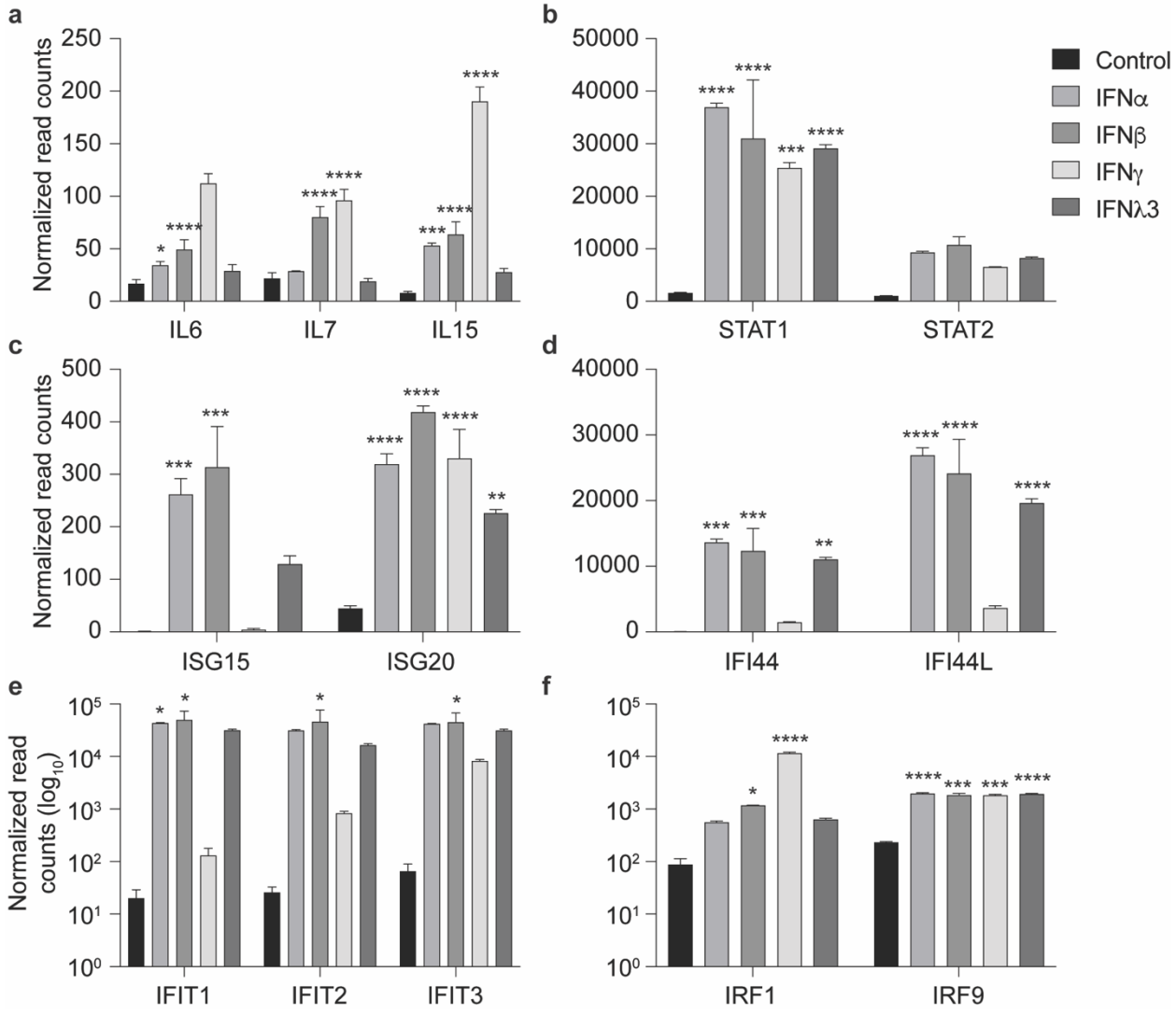

Supplementary Figure 2

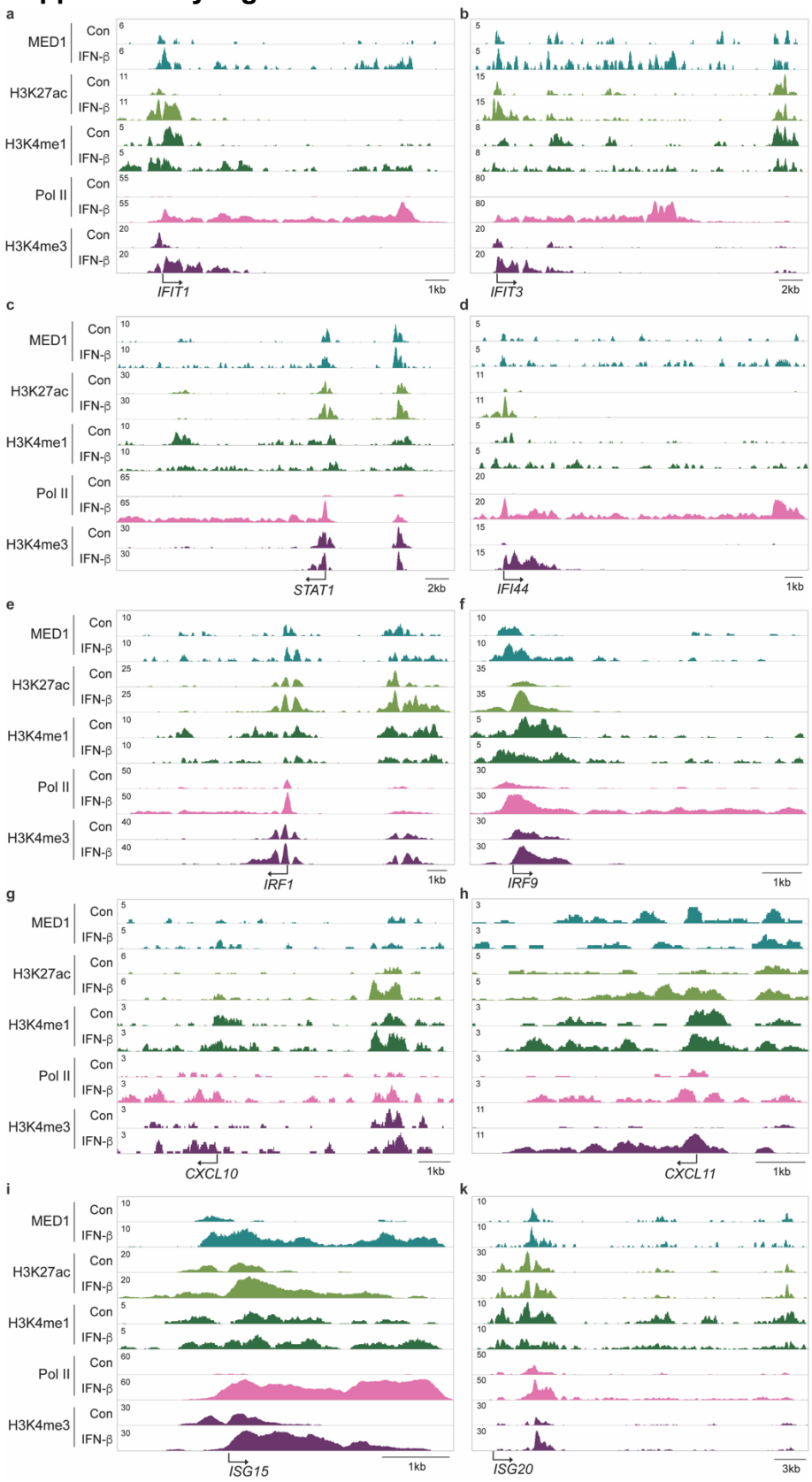

Supplementary Figure 3

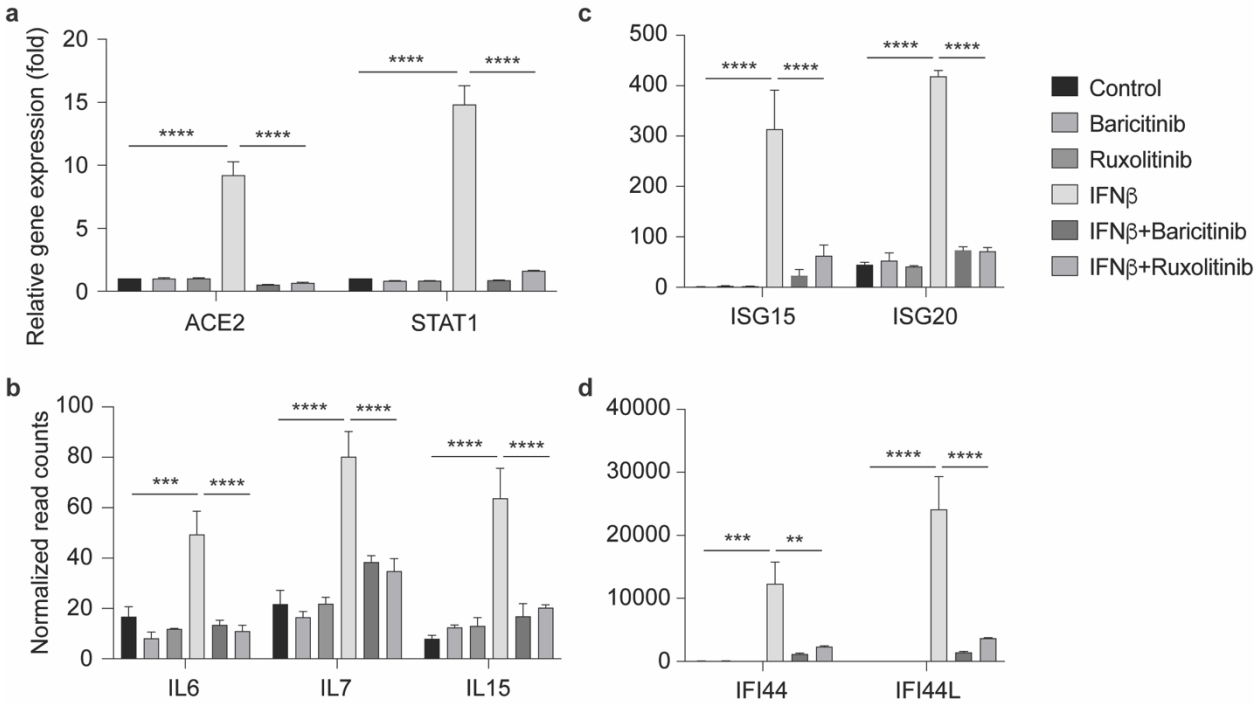
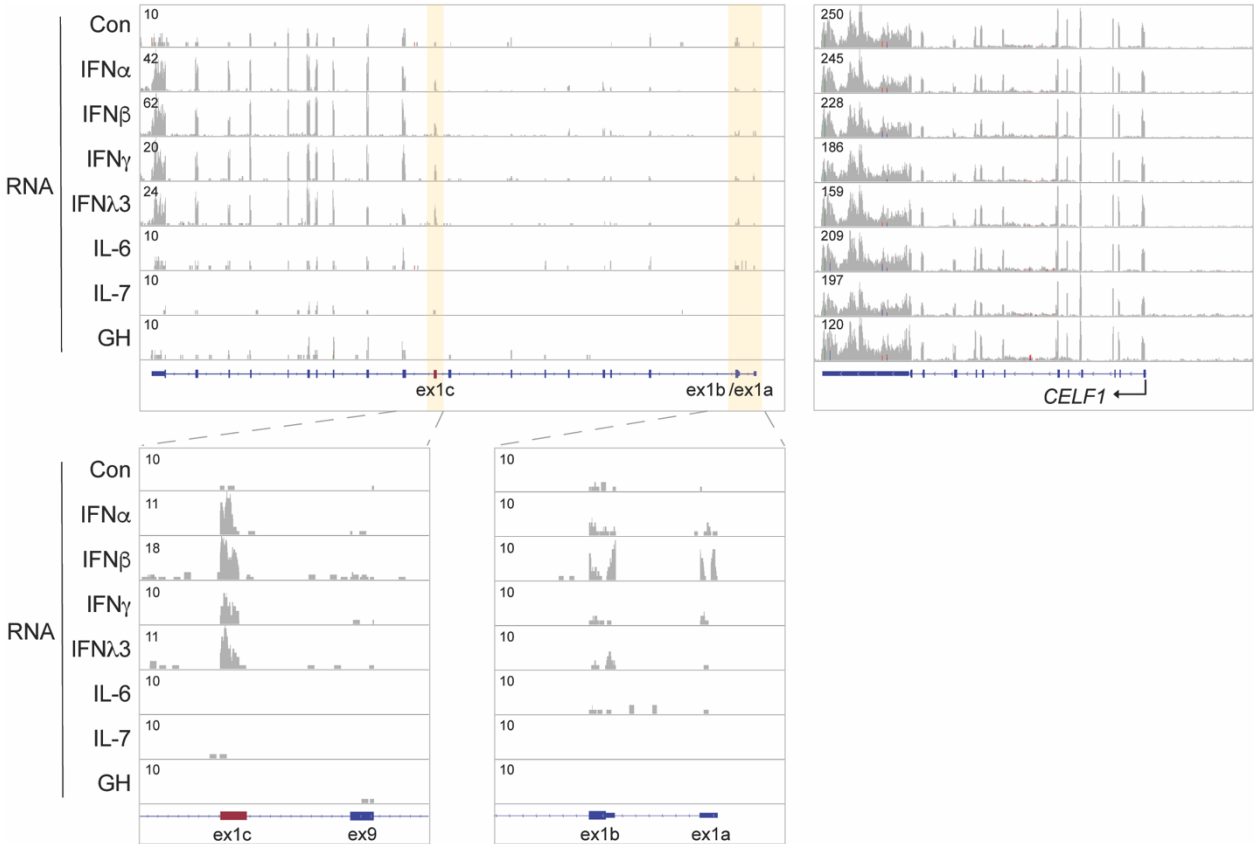
Supplementary Figure 4